CHEMBIOCHEM

DOI: 10.1002/cbic.200800609

Interactions of HIV-1 Antibodies 2F5 and 4E10 with a gp41 Epitope Prebound to Host and Viral Membrane Model Systems

Ana S. Veiga,[c] Leonard K. Pattenden,*[a, b] Jordan M. Fletcher,[a] Miguel A. R. B. Castanho,[c] and Marie Isabel Aguilar[a]

Two HIV-1 recognition domains for the human monoclonal antibodies (MAb) 2F5, which recognises the core sequence ELDKWA, and 4E10, which recognises the core sequence NWFNIT, serve as promising models for immunogens in vaccine development against HIV-1. However, the failure of these recognition domains to generate broadly reactive neutralizing antibodies, and the putative membrane-binding properties of the antibodies raised to these recognition domains, suggest that additional features or recognition motifs are required to form an efficient immunogen, which could possibly include the membrane components. In this study we used an extended peptide epitope sequence derived from the gp41 native sequence (H-NEQELLELDKWASLWNWFNITNWLWYIK-NH), which contains the two recognition domains for 2F5 and 4E10, to examine the role of model cell (POPC) and viral (POPC/cholesterol/sphingomyelin) membranes in the recognition of these two antibodies. By using a surface plasmon resonance biosensor, the binding of 2F5 and 4E10 to membranes was compared and contrasted in the presence and absence of prebound peptide epitope. The recognition of the peptide epitope by each MAb was found to be distinct; 2F5 exhibited strong and almost irreversible binding to both membranes in the presence of the peptide, but bound weakly in the absence of the peptide epitope. In contrast, 4E10 exhibited strong membrane binding in the presence or absence of the peptide epitope, and the binding was essentially irreversible in the presence of the peptide epitope. Overall, these results demonstrate that both 2F5 and 4E10 can bind to membranes prior to epitope recognition, but that high-affinity recognition of gp41-derived epitope sequences by 2F5 and 4E10 occurs in a membrane context. Moreover, 4E10 might utilise the membrane to access and bind to gp41; such membrane properties of 2F5 and 4E10 could be exploited in immunogen design.

Introduction

The viral envelope glycoprotein trimeric spikes responsible for the entry of the human immunodeficiency virus type 1 (HIV-1) into target cells is composed of heterodimeric units of surface glycoprotein gp120 and the transmembrane glycoprotein gp41 (reviewed in refs. [1–3]). The binding of gp120 to cellular receptors and subsequent changes within the gp41 ectodomain involve the formation of a six-helix bundle structure, and lead to both membrane fusion and viral entry.[1–4] The critical role of the envelope spikes has made inhibiting viral entry a viable approach for treating HIV infection by using peptides and small molecules (reviewed in ref. [5]), and the exposed nature of the envelope spikes facilitates their application as immunogens for raising neutralizing antibodies against HIV (reviewed in ref. [6]).

Within a vaccine approach, cross-clade neutralizing antibodies that induce both humoral and cellular immunity will have the greatest success in overcoming HIV persistence.[7] The human monoclonal antibodies (MAbs) 2F5 and 4E10 are two rare, broadly neutralizing antibodies against HIV-1[8–10] that interact with highly conserved epitopes close to the viral membrane surface termed the membrane proximal region (MPR) of gp41, which spans some 30 amino acids (amino acids (a.a.) 653–683 according to HXBc2 numbering). Specifically, these MAbs recognize epitopes in gp41 with core sequences ELDKWA (2F5, a.a. 662–667) and NWF(D/N)IT (4E10, a.a. 671–676).[9–14]

However, following immunisation in animals and humans these peptides alone have failed to generate broadly reactive neutralizing antibodies;[15,16] this suggests that additional features or recognition motifs are required to form an efficient immunogen.

An additional feature that might be required to form an immunogen is the viral membrane. It is believed that the binding affinity of 2F5 and 4E10 to the epitopes is enhanced when the peptides are in a lipophillic or membrane environment.[17–19] Indeed, based on the crystal structures of 2F5 and 4E10, it has

[a] *Dr. L. K. Pattenden, Dr. J. M. Fletcher, Prof. M. I. Aguilar*
Department of Biochemistry and Molecular Biology
Monash University, Clayton, Victoria, 3800 (Australia)

[b] *Dr. L. K. Pattenden*
Current address: School of Medicinal Sciences
(Health Innovations Research Institute)
Building 223, RMIT University
P.O. Box 71, Bundoora, Victoria 3083 (Australia)
Fax: (+61) 3-9925-7063
E-mail: leonard.pattenden@rmit.edu.au

[c] *Dr. A. S. Veiga, Prof. M. A. R. B. Castanho*
Instituto de Medicina Molecular, Faculdade de Medicina de Lisboa
Avenue Prof. Egas Moniz–Ed. Egas Moniz, 1649-028 Lisboa (Portugal)

been proposed that these MAbs can interact with the viral membrane through a hydrophobic surface present on the third complementarity-determining region of the heavy chain (CDR H3), which possibly facilitates binding to gp41 epitopes that lie close to the membrane.[18,20] Additional studies have shown that diverse lipid species can be recognised by 2F5 and 4E10, including both neutral and anionic phospholipids,[21,22] specialised anionic lipids, such as phosphatidylinositol-4-phophate (PtdIns(4)P),[23–25] and cardiolipin.[26] An overall conclusion that has been drawn from these studies is that the recognition of gp41-derived epitopes by 2F5 and 4E10 occurs in a membrane context.[22,27]

Surface plasmon resonance (SPR) is a key biophysical technique that can provide exquisite details of the kinetics and affinity of interactions between peptides, lipids, membranes and antibodies relevant to designing gp41-based immunogens.[14,24,27–34] However, despite advances in immunogen design, which have in part been achieved by using results of SPR-based analyses, the controversy in a key issue regarding epitope recognition by 2F5 and 4E10 has not been suitably resolved.[35]

The theory that the 4E10 MAb can bind to a membrane in the absence of an epitope is gaining wider acceptance. Indeed, 4E10 binding to the NWF(D/N)IT motif has been reported to follow a two-phase process of attachment to the membrane-bound epitope followed by a large conformational change to expose the complete epitope for strong binding.[34] However, despite early reports,[21,22,26] whether 2F5 MAb can bind to the membrane or whether the membrane has any involvement in 2F5 recognition of the ELDKWA motif, is a particular controversy. Of particular note, recent SPR studies suggest that the binding of 2F5 to the ELDKWA motif is completely independent of the membrane. Specifically, Scherer and colleagues observed no binding whatsoever for 2F5 on 4:1 phosphatidylcholine/cholesterol or 1:7:2 cardiolipin/phosphatidylcholine/cholesterol membranes.[32] In another study, little or no direct binding of 2F5 to virion-like membranes in the absence of the epitope was noted by SPR;[34] this was possibly due to the 2F5 epitope being predominantly solvent-exposed and distinct from the membrane. This might mean that 2F5 does not engage the membrane directly or that the ELDKWA motif does not require a membrane context whatsoever.[34]

A major question the field is still addressing is therefore the relevance of a lipid environment: whether the membrane is simply tolerated in binding to 2F5 and 4E10; or whether a lipid environment modulates gp41 epitopes to adopt a more structured (immunogenic) conformation, which is then recognised by the MAbs; or whether it is a combination of membranes enhancing the epitope structure as well as directly forming part of a combined lipid/peptide antigen. The implication of understanding the context of 2F5 and 4E10 recognition of their gp41 epitopes could lead to the development of more successful immunogens or biomolecular design for specific "tuning" of therapeutic antibodies based on 2F5/4E10 scaffolds.

In the present work, we examined the role of neutral cell- and viral-like membranes in the mechanism of action of these two MAbs. Specifically, the interactions of 2F5 and 4E10 were investigated in the presence and absence of a gp41 peptide that encompasses both 2F5 and 4E10 epitopes, and was prebound to model cell and viral membranes. We employed an SPR optical biosensor, which are increasingly used to directly study membrane-mediated interactions.[36] It was found that both 2F5 and 4E10 are able to bind to membrane surfaces, but 4E10 showed a comparatively greater affinity and faster dissociation rate. In the presence of the gp41 epitope prebound to membranes, both 2F5 and 4E10 bound by a two-state model and had considerably stronger—almost irreversible—association with the surfaces. Based on our findings we suggest that 2F5 binds to the epitope independently of the membrane, and that the membrane might be important to establishing an ordered structure of the epitope, and thereby facilitates recognition. We further propose that 4E10 recognises the gp41 epitope as a combined peptide/membrane antigen. These diametric properties of the MAbs are discussed in terms of immunogen design and new emerging strategies that can be undertaken in an attempt to raise neutralizing antibodies to HIV.

Results

We investigated the interaction of the HIV-1 MAbs 2F5 and 4E10 with model membranes using an SPR biosensor, which detects changes in the refractive index at the sensor surface caused by mass changes. Throughout the studies we used model membrane systems that mimic the conditions present on both the target cell and viral membranes. Liposomes composed of POPC (1-palmitoyl-2-oleyol-*sn*-glycero-3-phosphocholine) were used to mimic the target cell membrane as POPC is a zwitterionic lipid (i.e., neutral at the pH conditions used) with fluidity properties similar to biological membranes.[37] Liposomes composed of POPC/cholesterol (Chol)/sphingomyelin (SM; 1:1:1) were used as a neutral mimic of the viral membrane, which is rich in both Chol and SM[38,39] and has been used in similar ratios of 3:1:1[38,39] and 4.5:1:1[38,39] in other studies.

The SPR measurements examined several facets that are relevant to the recognition of the gp41 epitopes by 2F5 and 4E10. Firstly, membrane-only experiments were carried out to examine the binding of antibodies to membranes alone (no epitope), and secondly, epitope experiments were undertaken in which the binding of the antibodies to membranes preconditioned with the gp41 epitope was examined at three different epitope concentrations.

For both types of measurements, liposomes were immobilized on the surface of the sensor chips from 8389 to 10739 response units (RU) for POPC vesicles and 11109 to 14542 RU for POPC/Chol/SM vesicles. For membrane-only experiments, a dimethyl sulfoxide (DMSO) buffer control was undertaken prior to injecting the antibodies in order to ensure that these experiments were consistent with epitope experiments, as a small percentage of DMSO (0.14%, *v/v*) was critical for the solubility of the peptide epitope prior to membrane capture. These DMSO buffer injections caused very minor changes to either surface compared to the level of liposomal deposition (± 10 RU). The peptide epitope was prebound at 0.3, 0.5 or 1 μM

in DMSO, and elicited concentration-dependent changes in the refractive index measured, since capture levels ranged from 62 to 146 RU POPC surfaces and 32 to 118 RU for POPC/Chol/SM surfaces.

A schematic diagram of the assays is presented in Figure 1. Immediately following the control DMSO injection or peptide prebinding (60 s time delay), the MAbs were injected and their binding to the surfaces were determined. When MAbs were injected across the immobilized liposomes over a range of concentrations (0.06–0.3 μM for 2F5 and 0.06–0.5 μM for 4E10), the surface response, which reports protein binding to the membrane, was found to increase with higher protein concentrations. A fresh liposome surface was generated for each MAb binding test to prevent carry-over of bound material from influencing subsequent measurements.

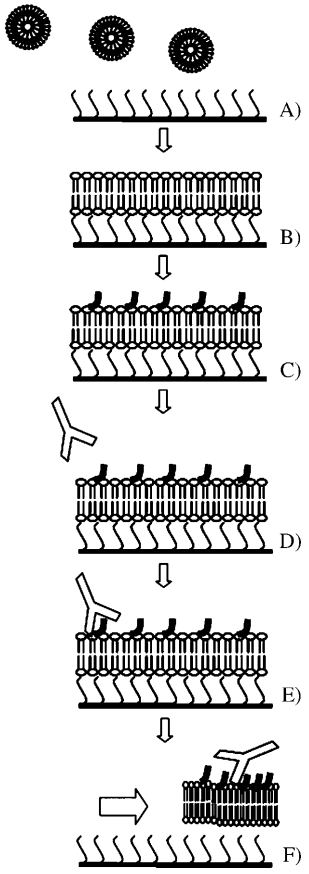

Figure 1. Schematic representation of the SPR experiments. The L1 chip consists of dextran modified with lipophilic compounds. A) Small unilamellar vesicles (SUVs; 50 nm) were applied to the sensor chip surface; B) liposomes adsorb to the surface spontaneously and form a supported lipid bilayer. C) To study monoclonal antibody (MAb) binding, membranes were preconditioned with the gp41 epitope. D) Monoclonal antibodies, 2F5 and 4E10, were introduced to the surface either without the epitope (shown in B) or following epitope capture (shown in D). E), F) After each binding assay the sensor surface was regenerated with the appropriate conditions.

2F5 and 4E10 membrane interactions in the absence of the gp41 epitope

Both 2F5 and 4E10 antibodies bound to the POPC (Figure 2A and B) and POPC/Chol/SM surfaces (Figure 2C and D) in the absence of the peptide epitope. The results obtained show a general increase in binding concomitant with increasing concentrations of both antibodies. However, in the case of 2F5 binding, the sensorgrams were not ideal with respect to both POPC and POPC/Chol/SM, and showed a decreasing response during the association phase and at lower concentrations (Figure 2A and B). In addition, the binding of 2F5 to both POPC and POPC/Chol/SM membranes did not return to baseline and resulted in the defined capture of 2F5 to the surfaces. A plot of response versus concentration at the end of the dissociation phase is shown in Figure 3, and demonstrates that the relative RU levels were similar for 2F5 on both POPC and POPC/Chol/SM; this suggests a similar affinity of 2F5 for these two lipid surfaces.

In contrast, higher binding levels were achieved for 4E10 binding to POPC and POPC/Chol/SM surfaces than for 2F5 (Figure 2C and D). In addition, higher binding levels were achieved for 4E10 on the POPC surfaces compared to POPC/Chol/SM in both the association and dissociation phases. The binding and dissociation levels were also proportionally distributed for POPC surfaces, but showed distinct groupings of concentrations on the POPC/Chol/SM surfaces. The plot of response versus concentration at the end of the dissociation phase shown in Figure 3, further demonstrates that 4E10 exhibited higher binding to POPC membranes compared to POPC/Chol/SM, and clearly shows there is much higher response achieved for 4E10 despite a smaller contact time for the injections than with 2F5.

The complexity of the interactions of these MAbs with the lipid-only surfaces (Figure 2) precluded kinetic fitting and steady-state approximations since the curves did not reach a plateau (Figure 3) even following extended injection times or higher concentrations of MAb (data not shown). In the case of 4E10, closer steady-state conditions were possible with extended injections or higher concentrations, however, such conditions required very harsh regenerations, which damaged the sensor chip surfaces and caused problems with consistency for assay replication. Despite not being able to fit simultaneously, dissociation-only fitting was possible for all experiments except 2F5 binding to POPC/Chol/SM, which had a relative increase over the fitted period due to baseline drift. Fitting was achieved for the other membranes by using the Langmuir model with global fitting of the apparent k_d from late in the dissociation phase ($t = 400$–650 s; highlighted in Figure 2A–D) when there was more of a 1:1 interaction. Although the calculation of apparent k_d values with the selected time window and model are not ideal, the behaviour of the MAbs on the membrane surfaces was consistent enough under these conditions to allow a comparison of the behaviour of the different MAbs and surfaces to a higher degree of analytical standards. The χ^2 and apparent k_d values are listed in Table 1 and demonstrate that despite the relative affinity being higher for 4E10, the rate of shedding of 4E10 from both POPC and POPC/Chol/SM is essentially the same, and is an order of magnitude faster than 2F5 for the POPC surface.

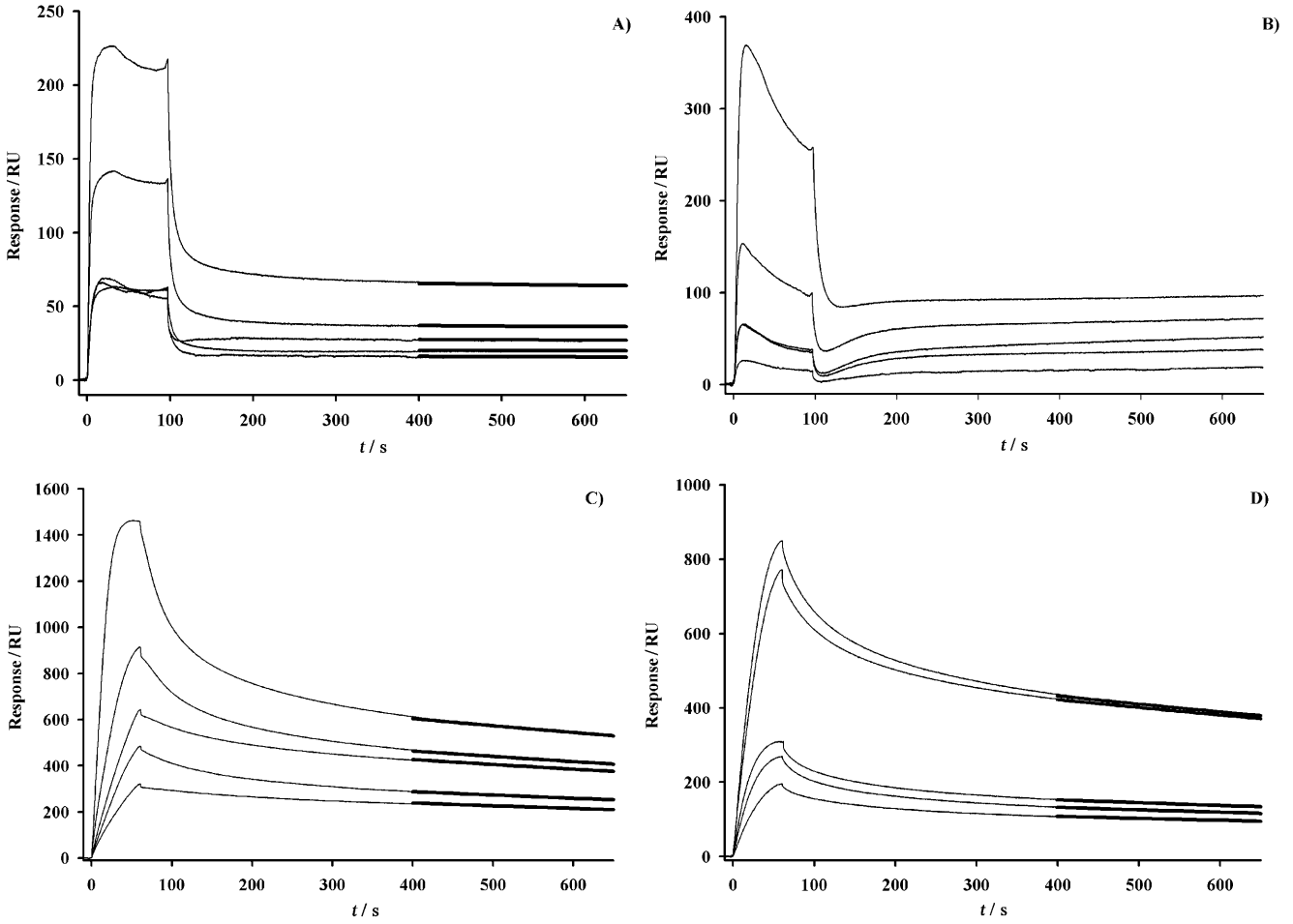

Figure 2. Sensorgrams obtained for 2F5 binding to immobilized A) POPC and B) POPC/Chol/SM (1:1:1) lipid membrane surface (L1 chip). Sensorgrams for the binding of 4E10 to immobilized C) POPC and D) POPC/Chol/SM. MAbs samples (0.06, 0.08, 0.1, 0.2 and 0.3 μM) were injected over a freshly prepared lipid surface, and subsequent association and dissociation were monitored. The Langmuir binding model was used to fit the data between 400–650 s.

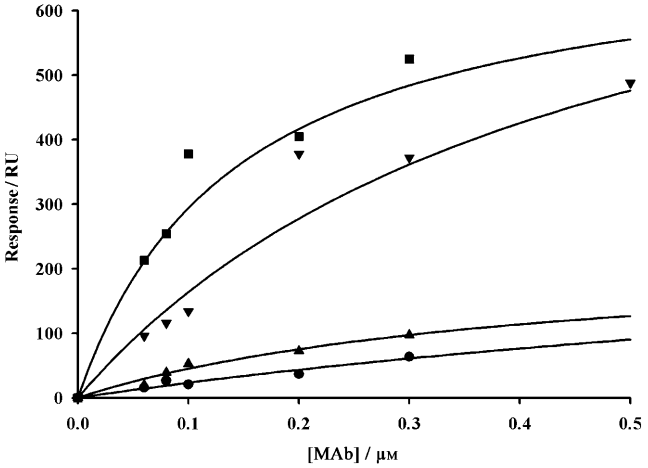

Figure 3. Plots of response units (RU) measured at $t = 700$ s versus the concentration of MAb for the binding of 2F5 and 4E10 to POPC and POPC/Chol/SM surfaces. Plots indicate 2F5 with POPC (●) and POPC/Chol/SM (▲); and 4E10 with POPC (■) and POPC/Chol/SM (▼).

Table 1. Apparent dissociation (k_d) rate constants for 2F5 and 4E10 binding to POPC and POPC/Chol/SM membranes, determined by numerical integration by using the Langmuir model.

	2F5		4E10	
	POPC	POPC/Chol/SM	POPC	POPC/Chol/SM
k_d [s^{-1}] × 10^{-6}	76.4	n.d.[a]	520	520
χ^2	0.165	n.d.[a]	4.42	0.979
residuals	±1	n.d.[a]	−2 to 8	−2 to 5

[a] n.d.: not determined.

2F5 and 4E10 membrane interactions in the presence of the gp41 epitope

To study 2F5 and 4E10 interactions with the membrane-bound peptide epitope, a selected range of peptide epitope concentrations (0.3, 0.5 and 1 μM) were prebound to the membrane before interactions were examined by using a range of concentrations of the MAbs (0.06–0.3 μM for 2F5 and 0.06–0.5 μM for 4E10). Figures 4 and 5 show the sensorgrams and kinetic fitting of the binding of 2F5 to the different concentrations of

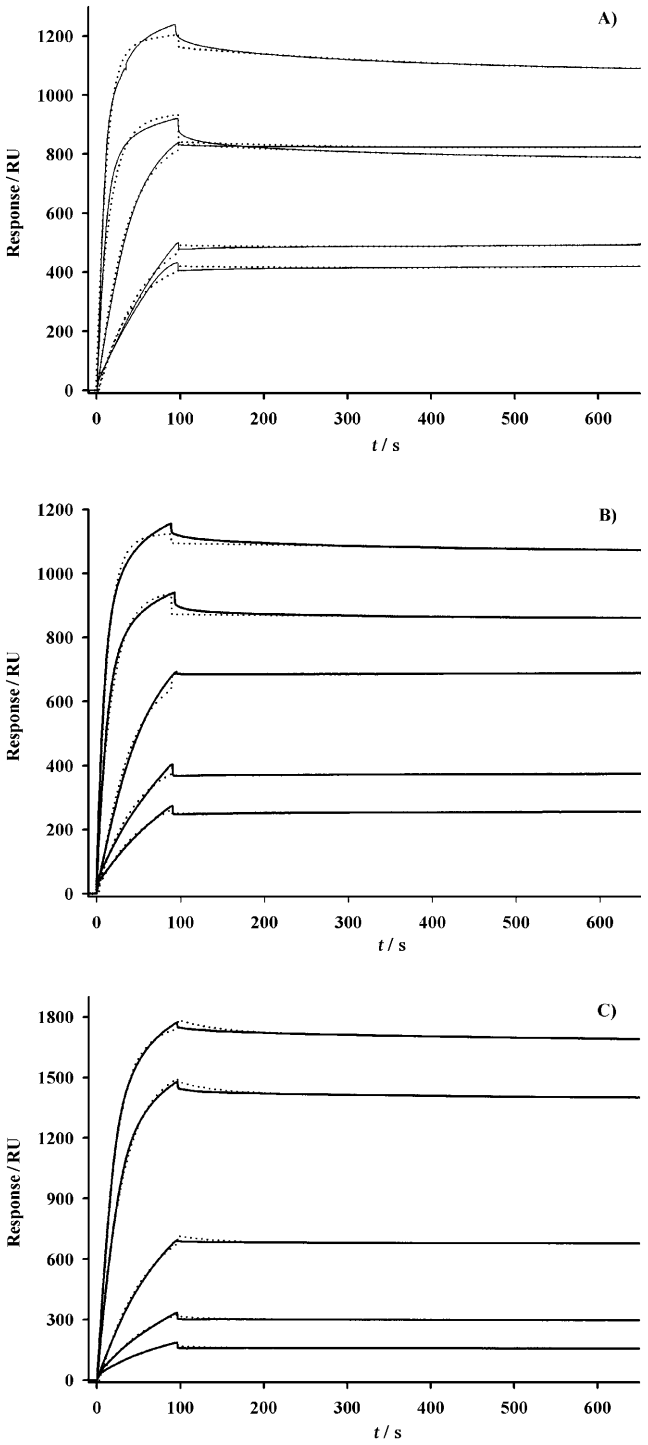

Figure 4. Sensorgrams obtained for 2F5 (0.06, 0.08, 0.1, 0.2 and 0.3 μM) binding to membranes of POPC on the L1 sensor chips in the presence of peptide epitope at: A) 0.3, B) 0.5, and C) 1 μM. The two-state binding model was used to fit the data (dotted lines).

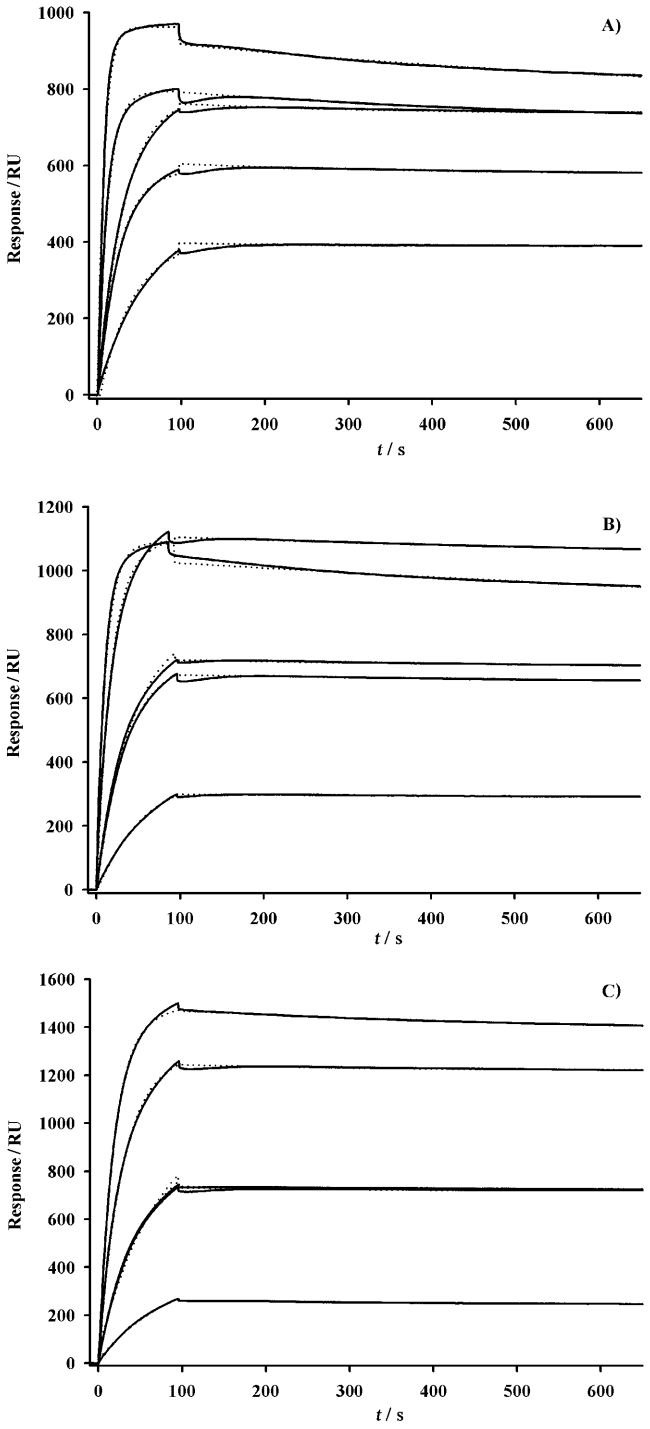

Figure 5. Sensorgrams obtained for 2F5 (0.06, 0.08, 0.1, 0.2 and 0.3 μM) binding to membranes of POPC/Chol/SM on the L1 sensor chips in the presence of peptide epitope at: A) 0.3, B) 0.5, and C) 1 μM. The two-state binding model was used to fit the data (dotted lines).

the peptide epitope precaptured to POPC and POPC/Chol/SM surfaces, respectively, and Figures 6 and 7 show the corresponding sensorgrams and curve fitting for 4E10 binding.

The capture levels of peptide (prior to MAb injection) ranged from 62 to 146 RU for POPC–epitope surfaces, and the values for 0.3 μM peptide (75 ± 13 RU) were slightly less than for 0.5 μM peptide (85 ± 17 RU), and both were less than with 1 μM peptide (125 ± 21 RU). The corresponding capture levels for POPC/Chol/SM–epitope ranged from 32 to 118 RU, and specific values for 0.3 μM peptide (51 ± 19 RU) were similar to 0.5 μM peptide (53 ± 12 RU), which were both less than with 1 μM peptide (89 ± 29 RU).

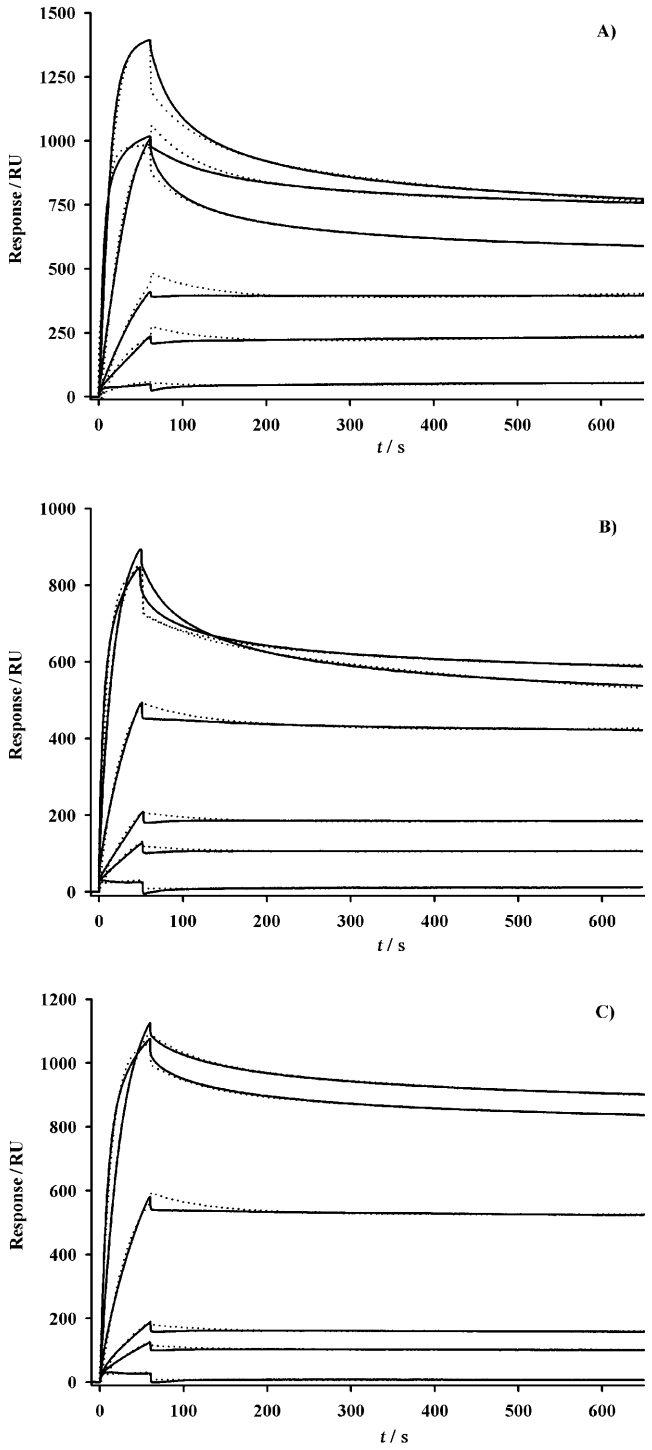

Figure 6. Sensorgrams obtained for 4E10 (0.06, 0.08, 0.1, 0.2, 0.3 and 0.5 μM) binding to immobilized POPC lipid membrane surface (L1 chip) in the presence of peptide epitope at: A) 0.3, B) 0.5, and C) 1 μM. The two-state binding model was used to fit the data (dotted lines).

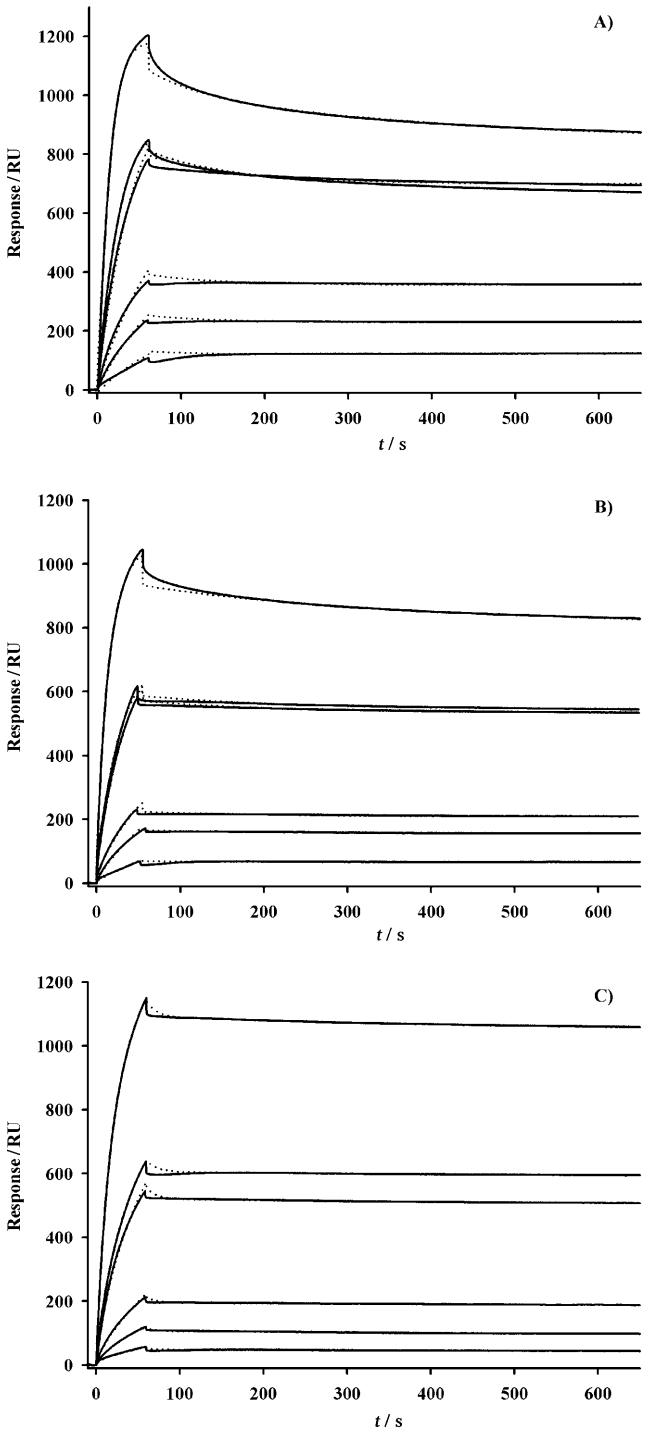

Figure 7. Sensorgrams obtained for 4E10 (0.06, 0.08, 0.1, 0.2, 0.3 and 0.5 μM) binding to immobilized POPC/Chol/SM lipid membrane surface (L1 chip) in the presence of peptide epitope at: A) 0.3, B) 0.5, and C) 1 μM. The two-state binding model was used to fit the data (dotted lines).

For subsequent MAb interactions with these surfaces, it is evident from Figures 4–7 that binding was so tight under all conditions that very little 2F5 or 4E10 dissociated from the peptide-bound surfaces; this reflects a very strong and almost irreversible association of MAbs in the presence of the peptide epitope for both membranes and all MAb concentrations studied. This contrasts quite dramatically to the binding of the MAbs to membranes alone (Figure 2 A–D).

Overall the sensorgrams show a generally higher MAb response at all concentrations in the presence of higher peptide epitope concentrations. The 2F5 sensorgrams have a better data spread than the 4E10 sensorgrams, which exhibited more

of a grouping at lower 4E10 concentrations. The 2F5 responses in the association and dissociation phases were: 166–1720 RU (association) and 157–1690 RU (dissociation) on the POPC–epitope surface; 250–1480 RU (association) and 246–1441 RU (dissociation) for the POPC/Chol/SM–epitope surface. These ranges contrast to the lower 4E10 responses of 12–1380 RU (association) and 7–902 RU (dissociation) for the POPC–epitope surface, and 60–1180 RU (association) and 44–1060 RU (dissociation) for the POPC/Chol/SM–epitope surface.

From these data ranges it can be seen that 2F5 exhibits higher affinity for the surfaces than 4E10, and a kinetic fit for all sensorgrams was possible with a two-state model. The two-state model was refined for fitting the data by setting the R_{max} as a local parameter to account for variability of captured peptide to the surfaces, and by including terms for baseline drift and mass transfer limitations. It was found that all peptide epitope concentrations gave similar rate constants for a given MAb, but the 1 μM peptide epitope experiments provided the lowest χ^2 values and displayed less variation than at other concentrations. Though these χ^2 values are generally higher than desired ranges for SPR experiments, the deviations from the fit might be a an imperfect behavioural property of the MAbs and membrane–epitopes to simplified models, or might reflect systematic deviations and noise due to high membrane capture levels as often found in membrane SPR experiments. However, deviations that cause elevated χ^2 values are predominantly found either at the end of the injection phase or at the very start of the dissociation phase, and the rest of the fitted areas have very little deviation from ± 1 RU; therefore the fitted data provide a close description of the two-state behaviour of MAbs on the membrane–epitope surfaces. The data obtained for 1 μM peptide epitope are therefore presented in Table 2 and the values for the K_A and K_D are reported as ranges that include all the 0.3, 0.5 and 1 μM data.

It can be seen that 2F5 displays approximately threefold higher affinity for membrane-captured epitope surfaces than 4E10, and there was essentially no difference in the affinity displayed for a particular lipid composition by either MAb. The values for 2F5 range from $K_A = (6–6.5 \times 10^8)\ M^{-1}$ to $(6.2–13 \times 10^8)\ M^{-1}$ for POPC–epitope and POPC/Chol/SM–epitope surfaces, respectively, whereas 4E10 has K_A values ranging from $(2.4–3 \times 10^8)\ M^{-1}$ and $(2.1–2.4 \times 10^8)\ M^{-1}$ for POPC–epitope and POPC/Chol/SM–epitope surfaces, respectively (Table 2). The slightly higher affinity constant (K_A) for the interaction of 2F5 with the POPC/Chol/SM–epitope was because the fitted data yielded much smaller and closer values for k_{a2} (s^{-1}) and k_{d2} (s^{-1}) at all peptide epitope concentrations. When changes in the parameter values, such as k_{a2} and k_{d2}, are small, they do not influence the closeness of the fit and can vary broadly in the fitting iterations; the BIAeval software often sets a value of the parameter that is beyond reasonable measurement ($\sim 10^{-6}$ for rate constants) and reports standard error values that are $>10\%$ for the parameter.[40] For the fit for 2F5 to POPC/Chol/SM–epitope surfaces, the standard error for k_{a2} and k_{d2} was $>10\%$, which indicates that changes in the k_{a2} and k_{d2} parameter values do not influence the closeness of the fit; this demonstrates that the interactions of 2F5 with the POPC/Chol/SM–epitope surface was more dependent on the values of k_{a1} ($M^{-1}\,s^{-1}$) and k_{d1} (s^{-1}) compared to 2F5 interactions with POPC–epitope or 4E10 interactions with either surface.

If the interaction of the MAbs with the peptide–membrane surface can be described in terms of a two-step process, then the values of k_{a1} and k_{d1} describe the initial interaction of the MAbs with the combined peptide–membrane immunogen, which is generally regarded to be mediated by electrostatic interactions with membranes[41] or peptide/proteins.[42] The k_{a1} values for the interaction of both MAbs with all peptide-bound surfaces are similar, with the exception of 4E10 interactions with the POPC/Chol/SM–epitope surface, which is twofold lower. Comparison of the values of k_{d1} for 4E10 reveal faster off-rates with the POPC/Chol/SM–epitope surface compared to the POPC–epitope surface, while the opposite was observed for 2F5, which exhibited a slower off-rate on the POPC/Chol/SM–epitope surface than the POPC–epitope surface. In addition, both 2F5 and 4E10 displayed similar k_{d1} values on the POPC–epitope surfaces.

The second association (k_{a2}) and dissociation (k_{d2}) rate constants can describe conformational changes to the peptide epitope, MAb or the subsequent insertion or reorientation of the MAb–peptide epitope within the membrane, which is largely mediated hydrophobic interactions (values listed in Table 2). To understand the importance of the second-state change to these MAbs it is meaningful to consider the *magnitude* of the k_{a2}:k_{d2} ratio in the two-state model, since mathematically this has an influence on the overall equilibrium constants. That is, when k_{a2} is proportionally larger than k_{d2}, the overall equilibrium constants will be significantly influenced by the rate of change of state in the system, and conversely when k_{a2} is proportionally smaller than k_{d2}, the overall equilibrium constants will be influenced far less by the rate of change of state in the system.

From Table 2, for 2F5 on the POPC–epitope surface this ratio

Table 2. Association (k_{a1}, k_{a2}) and dissociation (k_{d1}, k_{d2}) rate constants for 2F5 and 4E10 binding to POPC and POPC/Chol/SM membranes in the presence of the peptide epitope, determined by numerical integration by using the two-state model.

	2F5		4E10	
	POPC	POPC/Chol/SM	POPC	POPC/Chol/SM
k_{a1} [$M^{-1}s^{-1}$]$\times 10^5$	1.95	1.78	1.85	1.00
k_{d1} [s^{-1}]$\times 10^{-5}$	349	35.2	322	2570
k_{a2} [s^{-1}]$\times 10^{-6}$	18400	NR*[a]	11200	57300
k_{d2} [s^{-1}]$\times 10^{-6}$	1720	NR*[a]	2690	1070
K_A [M^{-1}]$\times 10^8$	6–6.5	6.2–13	2.4–3.0	2.1–2.4
$K_D \times 10^{-9}$	1.5–1.7	0.8–1.6	4.1–4.9	4.1–4.7
χ^2	21.9	31.2	21.9	2.6
k_t [$\times 10^8$]	13.8	342	5.69	764

[a] NR* has a standard error $>10\%$.

of k_{a2}/k_{d2} is ~10, whereas for 2F5 on the POPC/Chol/SM–epitope surface the magnitude differences are not significant to the fit and approximate to 1 with standard errors greater than 10%; the latter interaction—while obeying a two-state model—was not significantly dependent on the second rate constants for the quality of the fit and hence the values are not reported in Table 2. For 4E10 interactions with the POPC–epitope surface this ratio was ~4 with the slowest k_{a2} on-rate (and the fastest k_{d2} off-rate). For 4E10 on the POPC/Chol/SM–epitope surface the ratio was ~50, with the fastest k_{a2} on-rate (and slowest k_{d2} off-rate). This means that the second state transition is different for the particular MAb and is specific for the membrane environment; this suggests that 2F5 is less dependent on a membrane to effect strong binding, but might tolerate the involvement of a membrane the fluidity of which is less ordered. In the case of 4E10, we reason that not only is the involvement of the membrane important, but also a specific lipid species appears to influence the second state transition; however, these effects result in overall equilibrium constants that are almost the same for each MAb on the different membrane–epitope surfaces.

Discussion

2F5 and 4E10 are two MAbs against HIV-1, the epitopes of which are closely localized in the gp41 membrane proximal region (MPR), which is close to the viral membrane surface (the 2F5 epitope extends slightly outside the MPR N terminus). In the native state the MPR is believed to lie parallel to the surface of the viral membrane external layer. The 2F5 ELDKWA epitope motif has been shown structurally to be an independent and discrete extension from the viral membrane and forms the leg of the envelope spikes, which are attached to the 4E10 NWF(D/N)IT epitope foot that is continuous to the membrane plane. The MAbs have been modelled to dock in a manner by which they interact with both the membrane and peptide epitope.[43] In support of this, it has been proposed that the 2F5 and 4E10 MAbs interact with the viral membrane through a CDR H3 hydrophobic surface,[18,20] which is thought to orientate the MAbs in the manner proposed by Zhu et al.,[43] though we note that such a scenario as presented in this "tripod" structure of the viral envelope is not necessarily excluded in other "stalk" structural models.[44,45] Furthermore, previous studies have shown that the MPR has a tendency to partition into membranes,[46,47] and liposomal studies have shown that the binding of 2F5 and 4E10 to their epitopes is enhanced when gp41 is presented in a lipid environment.[17,18] However, despite this evidence, there remains no general consensus about the MPR structure in the context of the native gp120–gp41 or during the fusion process, and it is possible that this region is membrane-associated during the virus–cell fusion event.

The goal of the present study was to examine the membrane interactions of 2F5 and 4E10 by using POPC and POPC/Chol/SM liposomes as membrane models to mimic the host cell and viral membranes, respectively. The study was performed in the presence and absence of a peptide epitope (H-NEQELLELDKWASLWNWFNITNWLWYIK-NH), which has membrane-binding properties and contains both 2F5 (ELDKWA) and 4E10 (NWFNIT) epitopes flanked by native gp41 sequences. The use of this peptide epitope, rather than each MAb core epitope sequence separately, allows the binding properties of each MAb to be studied with the inclusion of the flanking residues that are naturally present in the whole gp41 envelope and provides a more relevant recognition context to better mimic the natural epitope conformation.

Currently, a powerful tool for determining the role of key peptide motifs and the relationships of sequence-specific properties to biological activity is the measurement of the underlying thermodynamics and kinetics of a specific interaction. One of the most commonly used optical biosensor technologies is SPR. Though other biophysical techniques provide important information on the relationship between membrane–peptide structures and biological function, SPR allows a detailed analysis of the kinetics and affinity of interactions and has been applied to the study of biomolecular interactions involved in almost every aspect of the HIV replication cycle.[48] However, there are only a limited number of SPR studies of 2F5 and 4E10 interactions with their epitopes that also involve the membrane, and experimental/kinetic details involving membrane interactions are incomplete and conflicting.[27,34]

We employed an SPR biosensor approach whereby liposomes of POPC or POPC/Chol/SM were deposited onto the L1 aliphatic alkanethiol-modified carboxymethyldextran surface to form suspended membrane surfaces that mimic biophysical aspects of the neutral cell- and viral-like membranes. The 2F5 and 4E10 MAbs were allowed to flow over the membrane surfaces in the absence or presence of prebound gp41 peptide epitope, and the binding was kinetically followed as a refractive index change proportional to a mass change on the surface.

The results obtained for the membrane-only experiments allow conclusions to be made about the membrane-binding characteristics of the MAbs. In agreement with other investigations,[21,22,26] we have found that not only 4E10, but also 2F5 can bind to membranes in the absence of gp41 peptide epitopes (Figure 2 A–D), although to a much lesser extent. Based on the low affinity of 2F5 for each membrane one may hypothesize that 2F5 binding to membranes alone might not necessarily involve the antigen-binding site where high-affinity interactions occur. This hypothesis is supported by previous fluorescence work,[49] in which it was shown that no extensive 2F5–membrane interaction occurred and thereby 2F5 was suggested not to use membrane interactions prior to high-affinity interaction and gp41 docking.

Higher binding responses were achieved for 4E10 on the POPC surfaces compared to POPC/Chol/SM or 2F5 on both surfaces, and the apparent off-rates from late in the dissociation phase show that the rate of shedding of 4E10 from both POPC and POPC/Chol/SM is essentially the same and is faster than 2F5. The low affinity interaction of 2F5 to membranes is in contrast to 4E10, which shows a much higher affinity for both membranes studied. This high affinity of 4E10 suggests that the antigen-binding site is likely to be involved, and therefore

the interactions of 4E10 with the membrane could be an important facet to immunogen design with this region of gp41.

The binding of 2F5 and 4E10 increased significantly in the presence of the membrane-bound peptide epitope complex and exhibited almost irreversible binding over the course of the measurements, that is, there was relatively little desorption during the dissociation phase. In the presence of the prebound epitope, we found that 2F5 binds with approximately threefold greater affinity for all surfaces than 4E10, with K_D values of 1.16–1.95 nM for 2F5 binding to POPC–epitope surfaces and 0.02–1.22 nM for POPC/Chol/SM–epitope surfaces, and K_D values of 0.63–5.69 nM for 4E10 binding to POPC–epitope surfaces and 0.54–4.21 nM for POPC/Chol/SM–epitope surfaces, which are similar to values determined by Alam et al. (K_D of 4 nM for 2F5 and 6 nM for 4E10 by ITC; 1.8 nM for 2F5 and 21.5 nM for 4E10 by SPR)[27] and Sun et al. (~10 nM reported for 4E10 by SPR).[34]

In terms of the mechanism of interaction, the two-state reaction model describes a more complex modification of the 1:1 Langmuir interaction, similar to the bivalent reaction model. For both models, the initial electrostatic binding of the MAbs to the peptide–membrane surface is followed by a second event, which could, in the case of the two-state reaction model, be a *rearrangement* or insertion of the MAb into the surface. For the bivalent model the second step is normally defined as the binding of the second antigen binding site. Our data show that there are at least two steps that could include bivalency, for which the involvement of the second antigen binding site might be a very fast process and be enhanced by the first antigen binding. owever, the very strong and/or irreversible binding of the MAbs to the peptide–membrane complex is consistent with an insertion or reorientation of the MAbs into the plane of the membrane upon binding and is mediated by hydrophobic interactions.

Conversely, 4E10 interactions with the peptide on the POPC/Chol/SM–epitope surface is far more dependent on the second rate constants to fit to the two-state model, with the fastest on-rate and slowest off-rate of all the assays for the second rate constants (k_{a2} and k_{d2}), but slowest on-rate and fastest off-rate for the first rate constants (k_{a1} and k_{d1}). This suggests that the membrane composition is important, since 4E10 does not show as good an initial interaction to the POPC/Chol/SM–epitope surface as to other surfaces, and curiously, the 4E10 POPC–epitope surface had 20% of the k_{a2} rate and twice the dissociation rate k_{d2}. This suggests that 4E10 exhibits strongest interactions with both the membrane and the peptide epitope as a combined peptide–membrane immunogen, and so lipid composition could be very relevant to 4E10 neutralisation.

These suggestions are supported by structural data. In terms of the structure of the peptides within membrane mimetic environments, an MPR synthetic peptide has been shown to adopt a helical conformation parallel to the membrane, near the lipid interfacial region,[50] and a revised structure has shown that the 2F5 and 4E10 immunogens are helical domains separated by a defined kink.[34] In contrast, the X-ray crystal structure of the 2F5 and 4E10 Fab (fragment, antigen binding) regions complexed to synthetic epitopes[18,20] demonstrate that the epitopes adopt a β-turn and α-helical conformation, respectively, that is distinct from the conformations found in the solution-based studies.[34,50] While the crystallographic evidence lacks a membrane context, the different structures suggest that each epitope might undergo a conformational change during recognition by the respective MAbs.

Given the proximity and location of the 2F5 and 4E10 epitopes to the viral membrane, it is not surprising that both MAbs bind almost irreversibly to the peptide in the membrane context. Based on the neutralising activity of each MAb, it could be anticipated that the MAbs would bind more strongly to the lipid composition of the model viral membrane with the peptide epitope (POPC/Chol/SM–epitope) than to the model mammalian membrane with the peptide epitope (POPC–epitope). However, since the binding of each MAb was similar with both lipid mixtures in the presence of the peptide epitope, the results suggest that the lipid composition requires further optimisation to provide a more precise mimic of the virion membrane. Indeed, other studies have shown that 2F5 and 4E10 bind unspecifically to neutral and anionic phospholipids (phosphatidylcholine (PC) and phosphatidylglycerol (PG) for 2F5 and PC, SM, phosphatidylethanol (PE), PG and phosphatidylserine (PS) for 4E10), and bind more strongly to CL.[21,22,26] It has also been reported that 4E10 might bind to PtIns(4)P through a phosphate-binding subsite,[23,24] and lipids, such as PS or PtIns(4)P, might be exposed at the HIV surface.[25] Additionally, Chol also seems to be important for 4E10 epitope recognition[51] and this could be the reason why the second rate constants obtained in the present study for the POPC/Chol/SM–epitope mixture exhibit different properties compared to the POPC–epitope surfaces. It is possible that Chol changes the fluidity of the acyl chains and the orientation of the phospho-head groups of the viral membrane and facilitates surface orientation of the peptide by tryptophan insertion at the interface;[34] this would give 4E10 an overall preference for cholesterol-containing lipid compositions combined with the gp41 epitope.

Naturally the exact composition of the HIV virion is controversial and might well be plastic to cell-type and cell-cycle specifics, which can alter lipid compositions at the site of budding (e.g., lipid rafts),[52] but more importantly the lipid composition in the vicinity of the gp41 spikes is unknown and it is feasible to speculate that the virion could have an asymmetric lipid distribution about the local environment of gp41, which would be facilitated or even dictated by envelope proteins as well as lipid concentrations at the site of budding. If so, the lipid environment and composition itself could play a critical role in the viral fusion process, and perhaps facilitate virion structural changes at the point of fusion or assist translocation due to the presence of localised inner leaflet lipids, such as SM and PtdIns-species.

Immunogen design

The gp41 epitopes have attracted increasing attention as promising models for immunogens in vaccine development (e.g., see ref. [53]). Phogat and Wyatt describe a range of strat-

egies currently undertaken to design either protein or peptide immunogens for HIV vaccines.[6] In the case of the 2F5 and 4E10 peptide epitopes this has frequently involved constraining or restricting peptide conformations and creating scaffold or carrier-assisted immunogens that try to present the peptide epitopes in a manner that elicits an immunogenic response relevant to native HIV envelope spikes.[6] Such approaches require characterisation of the molecular details of 2F5 and 4E10 interactions with the gp41 peptide epitopes, and an important consideration in these approaches is the role of the viral membrane, which—if important to recognition by MAbs—could be central to novel biomolecular design approaches and for presenting more biologically relevant immunogens.[25,35] An important question, therefore, concerns the role the membrane plays in MAb recognition. Though recent work may call into question whether 2F5 really binds phospholipid species,[32,34,54] very valid points have been raised that these differences could be merely technical, technique-specific or related to the phospholipid occupying only a small portion of the 2F5 antigen-binding paratope.[35] Recent work has shown that the conformation of the epitope recognised by the MAbs is a transient intermediate that conceivably might not be achievable with particular peptide lengths or lipid compositions, which do not present (in the case of 2F5) an extended, prehairpin intermediate conformation.[55] Therefore, such differences could also be a reflection of difficulties in studying the fine details of HIV biology.

Similarly the tryptophan-rich conserved region below the 2F5 domain (including the 4E10 epitope) can be functionally replaced with antibacterial peptides with similar membrane-perturbing properties as the 4E10 epitope; these may even contain strategic helix-breaking proline residues.[56] This indicates that the conformation of the MPR about the 4E10 epitope is more complex than current structural data suggest, and the membrane-perturbing properties are of paramount importance for function. Furthermore, the authors suggest that based on current structural data the MPR needs to also transition through short-lived intermediate conformations to attain the prefusion state.[56]

Indeed the Wyatt group have recently reported a fused hepatitis B S1–MPR (HBsAg–MPR) virus-like particle and examined different surface antigen contexts arranged on the hepatitis B S1 scaffold that comprises MPR-containing epitopes and plasma membrane/synthetic derived lipid constituents.[57] In this study the membrane was shown to be critical to recognition by delipidation and reconstitution of particles in 1,2-dioleoyl-*sn*-glycero-3-phosphocholine/1,2-dioleoyl-*sn*-glycero-3-phospho-L-serine (7:3). Curiously the MPR C-terminal constructs were most effective, which actually places the 2F5 portion of the epitope close to the membrane, and suitable 4E10 recognition was obtained only upon addition of transmembrane sequences C-terminal to the 4E10 portion of the epitope.[57] The authors attribute the extended transmembrane requirements to a more intimate association with the membrane, which could conceivably be brought about by a relaxation of the highly strained membrane (22 nm particles), or asymmetry of the membrane about the additional transmembrane extension to allow the membrane-perturbing properties of the MPR to structurally occur. The delipidation/lipidation properties of this new HBsAg–MPR platform, offers a means of experimentally investigating the lipid environment and novel lipids (or other nonlipid agents) for the HIV membrane, which could help achieve a more antigenic prehairpin structure. Conceptually this could be simply probed by using SPR and immobilised MAbs or Fab fragments for a more complete understanding of the lipid environment and role of the membrane in efficient antibody neutralisation.

Conclusions

Here, we have presented the significant finding that 2F5 does not bind specifically to the membrane, but the membrane is important to the secondary structure of the 2F5 epitope, presumably by supporting the epitope in the required prehairpin intermediate conformation recognised by 2F5. Conversely, we have shown 4E10 appears to bind to both the peptide and membrane, most likely as a combined immunogen, and therefore the composition of the membrane is predicted to be important for recognition. These important roles for the viral membrane about the peptide epitopes are a facet of HIV behaviour that could be exploited in novel immunogen design approaches to raise antibodies that are specific to HIV and that recognise both the viral membrane and part of gp41.

Experimental Section

General: (2-(1*H*-7-Azabenzotriazol-1-yl)-1,1,3,3-tetramethyl)uronium hexafluorophosphate (HATU), *N*-methyl pyrrolidone (NMP), dimethylformamide (DMF), diisoproylethylamine (DIPEA), piperidine, triisopropylsilane (TIPS) and trifluoroacetic acid (TFA) were of peptide synthesis grade and obtained from Auspep (Melbourne, Australia). POPC (1-palmitoyl-2-oleyol-*sn*-glycero-3-phosphocholine) was purchased from Avanti Polar-Lipids (Alabaster, AL, USA). Sphingomyelin (SM; chicken egg yolk), cholesterol (Chol), (3-[3-cholamidopropyl)dimethylammonio]-1-propanesulfonate (CHAPS) and sodium dodecyl sulfate (SDS) were obtained from Sigma (St. Louis, MO, USA). HEPES was obtained from Sigma (Castle Hill, NSW, Australia) and NaCl was from Amresco (Solon, Ohio, USA). HEPES buffer (10 mM HEPES buffer pH 7.4, 150 mM NaCl) was used throughout the studies by dilution from a 10× stock. The SPR system used was a BIACORE T100 analytical system (Biacore, Uppsala, Sweden) with L1 sensor chips (Series S; Biacore) for liposome attachment. The regeneration solutions were SDS (0.5%, *w/v*), CHAPS (20 mM), NaOH with methanol (10 mM NaOH, 20% MeOH) and NaOH (10 mM). All solutions used in the T100 were freshly prepared and filtered (0.22 μm filter).

Antibodies: Human HIV-1 gp41 monoclonal antibodies 2F5 and 4E10 from Dr. H. Katinger and Polymun Scientific were provided by the EU Programme EVA Centralised Facility for AIDS Reagents, National Institute for Biological Standards and Control (UK), and were also purchased from Polymun Scientific (Vienna, Austria). The MAbs 2F5 and 4E10 (100–670 μL) were dialysed in HEPES buffer (1 L, for >16 h, 4 °C) by using a SnakeSkin™ pleated dialysis tubing (10 kDa, Pierce, Rockford, IL, USA). The MAbs were diluted to ~tenfold prior to dialysis to reduce the protein concentration and avoid protein aggregation; no evidence of aggregation was detected in

samples by measuring absorbances at 280 and 320 nm, even after periods of more than six months after the experiments. Protein concentrations for assays were quantified with the modified Lowry, DC protein assay (Bio-Rad, Gladesville, NSW, Australia). In order to avoid signal response variations during the SPR experiments due to the differences between the MAb solutions and the running buffer, the dialysis buffer was subsequently filtered (0.22 μm membrane, Pall Life Sciences, Melbourne, Australia) and used as running buffer in SPR experiments, thereby removing refractive index changes between solutions. Refractive index differences between different MAb preparations was <2 RU.

Peptide synthesis: Rink amide resin was obtained from Novabiochem (San Diego, CA, USA) and Fmoc-L-amino acids were obtained from GL Biochem (Shanghai, China). The peptide H-NEQELLELDK-WASLWNWFNITNWLWYIK-NH (hereafter referred to as peptide epitope) was synthesised on Rink amide resin (on a 0.1 mmol scale) by using a Liberty™ microwave peptide synthesiser (CEM™; NC, USA) by employing Fmoc solid-phase techniques (for a review see ref. [58]). The peptide epitope was assembled by systemically repeated steps of "double" coupling and "double" deprotection. "Double" coupling: Fmoc-amino acid (5 equiv), HATU (4.5 equiv), DIPEA (10 equiv), in NMP (2×5 min, with 20 W microwave irradiation at 75 °C). "Double" deprotection: piperidine (20%) in NMP (1× 30 s, with 40 W irradiation at 38 °C; followed by 1×3 min, with 40 W irradiation at 75 °C).

Following linear assembly, the peptide was cleaved from the resin with simultaneous removal of side-chain protecting groups by treatment with a cleavage cocktail (2 mL) consisting of TFA (95%), TIPS (2.5%) and H_2O (2.5%) for 3 h at room temperature. Suspended resin was removed by filtration and the peptide precipitated in ice-cold diethyl ether. Solid material was then collected in a sintered glass funnel (pore size 4), washed with diethyl ether, dissolved with MeCN/H_2O (1:1) and lyophilised. An initial analysis of the crude material by RP-HPLC and mass spectrometry suggested the presence of multiple N-carboxy groups, which presumably resulted from the incomplete removal of *tert*-butoxycarbonyl side-chain protection from the indol nitrogen of the five tryptophan residues present.[59] Decarboxylation of these carbamic acid intermediates was achieved by dissolving the crude material in MeCN/H_2O/CH_3COOH (9:9:2) and stirring at room temperature, overnight. The peptide was then purified by preparative RP-HPLC by using an Agilent HP1100 system fitted with a Vydac™ C18 (250×22 mm) RP column. The eluents used were TFA (0.1%) in H_2O (A) and TFA (0.1%) in MeCN (B); the peptide was eluted by applying a linear gradient (6 mL min^{-1}, 0% to 60% B over 60 min). Fractions collected were examined by analytical RP-HPLC and those found to exclusively contain the desired product were pooled and lyophilised. Analysis of the purified final product by RP-HPLC indicated a purity of >90%. Successful synthesis was confirmed by electrospray-ionisation mass spectrometry (found: 3652.8; calcd: 3650.8).

Peptide preparation for biosensor experiments: Peptide stock solutions were prepared in DMSO and diluted to the desired concentrations with HEPES buffer. The total DMSO concentration was maintained at 0.14% (*v*/*v*) in the peptide samples throughout the SPR experiments to aid peptide solubility, as low DMSO concentrations are reported not to perturb particular liposomal compositions.[60] This value is well below the chemical compatibility of the L1 sensor chips (10%) and was confirmed not to cause large baseline changes in this study with buffer-only injections over membrane surfaces (±10 RU). Peptide concentrations were quantified with the modified Lowry, DC protein assay, and peptides were spectrophotometrically monitored for solubility and aggregation by measuring absorbances at 280 and 320 nm.

Liposome preparation and lipid bilayer formation: Small unilamellar vesicles (SUVs) of POPC and a mixture of POPC/Chol/SM (1:1:1) were used throughout the studies. POPC (dissolved in chloroform) alone or mixed with Chol (in chloroform) and SM (in chloroform/methanol mixture 2:1, *v*/*v*) was dried under a gentle stream of nitrogen. Solvent removal was completed in vacuo, overnight. The lipid was suspended in HEPES buffer (final concentration 1 mM) and sized by being subjected to seven repeated freeze/thaw cycles and extrusion (19 times) through polycarbonate filters (50 nm pore diameter).

All biosensor experiments were conducted at 25 °C with sample injections by using instrument high-performance parameters and collection rates (10 Hz). The L1 sensor chip surface was washed as part of a start-up cycle by the sequential injection of CHAPS (20 mM, 5 μL min^{-1} flow rate, 60 s contact time), NaOH in methanol (10 mM NaOH in 20% MeOH, 50 μL min^{-1}, 36 s) and NaOH (10 mM, 50 μL min^{-1}, 36 s). SUV were captured onto the L1 surface at a flow rate of 2 μL min^{-1} (2400 s). A NaOH pulse was used to remove loosely bound liposomes from the surface (10 mM, 50 μL min^{-1}, 36 s), which resulted in a stable baseline.

2F5, 4E10 and gp41 epitope scouting conditions: To establish the conditions of the binding experiments, scouting experiments were performed to optimise the MAbs and gp41 epitope concentrations (with varied amounts of DMSO), contact times and flow rates for capture of the epitope and subsequent antibody binding. It was found that only a narrow range of conditions was applicable to both POPC and POPC/Chol/SM surfaces with both antibodies. Extending beyond these conditions proved too detrimental to the membrane systems in terms of DMSO effects and regeneration of the surfaces; the latter was particularly difficult with elevated antibody concentrations or prolonged contact times, which needed to be optimised individually for 2F5 and 4E10. A range of solvents and additives were tested to increase the range of conditions, but only very harsh regeneration conditions—above the rigors typically employed for membrane systems (i.e., *n*-octyl-β-D-glucopyranoside or CHAPS regenerations)—successfully restored basal responses without carryover to subsequent assay cycles.

Scouting experiments examined various 2F5 and 4E10 concentrations (0.01–0.5 μM), gp41 epitope concentrations (0.1–1 μM), DMSO concentrations for dissolving the gp41 epitope (0.015–0.14% DMSO), contact times for each parameter (30–180 s) and flow rates for each step (5–30 μL min^{-1}). Regeneration conditions were screened by using a range of concentrations of solvents, detergents and additives comprising: SDS, polyethyleneglycol, polyethyleneimine, methyl-α-D-glucopyranoside, L-α-*o*-benzylglycerol, *n*-octyl-β-D-glucopyranoside, $MgCl_2$, EDTA, CHAPS and NaOH in methanol. The final conditions derived (detailed in the following section) provided the most reproducible results on the T100 biosensor platform.

2F5 and 4E10 binding to membranes or precaptured gp41 epitope: Solutions of 2F5 (0.06–0.3 μM) and 4E10 (0.06–0.5 μM) in HEPES buffer were studied on membrane surfaces prepared from the deposition of POPC or POPC/Chol/SM SUV (1 mM). The MAb experiments were performed either in the absence or presence of peptide epitope (concentrations of 0.3, 0.5 and 1 μM) prebound to the membrane surfaces. As control, MAb binding was studied in the presence of DMSO (0.14%, *v*/*v*) buffer control, as DMSO was critical for the solubility of the peptide epitope. Prebinding of the peptide epitope (or DMSO control treatment) was achieved by in-

jection of solutions over the membrane surfaces (5 μL min^{-1}, 180 s). Upon completion of the injection, the flow was continued (5 μL min^{-1} for 60 s) before the MAb solutions were injected over the combined membrane–epitope (or membrane–DMSO control) surfaces. The MAb solutions were injected by using different contact times at a constant flow (5 μL min^{-1}; 2F5 contact time 90 s, 4E10 contact time 60 s), followed by a uniform dissociation time (600 s). After each MAb binding assay, the sensor surface was regenerated (0.5%, *w/v*, SDS, 5 μL min^{-1}, 60 s), followed by the sequential injection of CHAPS (20 mM, 5 μL min^{-1}, 60 s), NaOH in methanol (10 mM NaOH in 20% MeOH, 50 μL min^{-1}, 36 s) and NaOH (10 mM, 50 μL min^{-1}, 36 s).

Analysis and data fitting: Analysis and fitting was conducted by using BIAeval version 4.1, Sigmaplot version 2001 and Graphpad Prism version 4.00. Because fitting the MAb interactions to the lipid-only surfaces with kinetic fitting or steady-state approximations was not possible, a comparative kinetic fit was used by global fitting of the dissociation phase ($t = 400$–650 s) to derive apparent values of the dissociation rate constant k_d as opposed to kinetically measured values obtained in the presence of the epitope. At the fitted period the dissociation phase was more uniform across both MAbs and membrane surfaces and demonstrated a more 1:1 Langmuir behaviour; this allowed a closer fit with lower χ^2 values and residuals.

For the MAb interactions with peptide epitopes, data were originally assessed for fitting to Langmuir 1:1 models as the simplest interaction before examination of fitting to bivalent (accounting for both interacting arms of the IgG molecules) and two-state reaction models (including modified models to account for possible mass transfer limitations or baseline drift). The bivalent model was rejected for two reasons: firstly it was found that the χ^2 values were generally higher; secondly, the fitting could be artificially manipulated to more closely match the data by setting high starting parameters—especially, any incremental value from 1×10^4–1×10^5 for k_{a1} (it should be noted that the bivalent model multiplies k_{a1} by a factor of two as part of the fit, which might have been relevant in this case). Such high initial parameters sometimes returned final values of k_{a1} beyond the range of the T100 SPR to accurately measure, and in some fits early iterations would automatically find a high value for k_{a1}; so, although the fit always appeared to match the data, the final numbers did not necessarily represent the true physicochemical properties of the MAbs.

The two-state model was refined by setting the R_{max} as a local parameter and making kinetic allowance within Biaeval 4.1 for systematic baseline drift (local parameter) and mass transfer limitations (global parameter), as used in the standard models for 1:1 binding with drifting baseline and 1:1 binding with mass transfer. The data could be fitted to this model, which provided lowest χ^2 values and consistent final numbers irrespective of initial values for the fitted parameters in the model.

Kinetic data were assessed by using χ^2 values, plots of the residuals from the model fitting and the significance of a parameter assessed by the standard error (SE) statistics. The quality of the fit to a specific parameter was deemed significant if the standard error was less than 10%. Except where specifically indicated, all parameter values were significant to the fit.

Acknowledgements

This project was partially funded by FCT-MCTES (Portugal), including a grant (SFRH/BD/14336/2003) under the program POCTI to A.S.V. Bifonds travel allowance is also acknowledged. Monoclonal antibodies 2F5 and 4E10 were provided by Dr. Hermann Katinger and Polymun Scientific, through the NIBSC Centralised Facility for AIDS Reagents supported by EU Programme EVA and the UK Medical Research Council. The support of the Australian Research Council is also acknowledged.

Keywords: antibodies · immunogen design · membrane proteins · membranes · surface plasmon resonance

[1] D. C. Chan, P. S. Kim, *Cell* **1998**, *93*, 681.
[2] R. Wyatt, J. Sodroski, *Science* **1998**, *280*, 1884.
[3] D. M. Eckert, P. S. Kim, *Annu. Rev. Biochem.* **2001**, *70*, 777.
[4] C. C. LaBranche, G. Galasso, J. P. Moore, D. P. Bolognesi, M. S. Hirsch, S. M. Hammer, *Antiviral Res.* **2001**, *50*, 95.
[5] S. Liu, S. Wu, S. Jiang, *Curr. Pharm. Des.* **2007**, *13*, 143.
[6] S. Phogat, R. Wyatt, *Curr. Pharm. Des.* **2007**, *13*, 213.
[7] D. R. Burton, R. C. Desrosiers, R. W. Doms, W. C. Koff, P. D. Kwong, J. P. Moore, G. J. Nabel, J. Sodroski, I. A. Wilson, R. T. Wyatt, *Nat. Immunol.* **2004**, *5*, 233.
[8] A. Trkola, A. B. Pomales, H. Yuan, B. Korber, P. J. Maddon, G. P. Allaway, H. Katinger, C. F. Barbas, D. R. Burton, D. D. Ho, J. P. Moore, *J. Virol.* **1995**, *69*, 6609.
[9] G. Stiegler, R. Kunert, M. Purtscher, S. Wolbank, R. Voglauer, F. Steindl, H. Katinger, *AIDS Res. Hum. Retroviruses* **2001**, *17*, 1757.
[10] M. B. Zwick, A. F. Labrijn, M. Wang, C. Spenlehauer, E. O. Saphire, J. M. Binley, J. P. Moore, G. Stiegler, H. Katinger, D. R. Burton, P. W. Parren, *J. Virol.* **2001**, *75*, 10892.
[11] T. Muster, F. Steindl, M. Purtscher, A. Trkola, A. Klima, G. Himmler, F. Ruker, H. Katinger, *J. Virol.* **1993**, *67*, 6642.
[12] C. E. Parker, L. J. Deterding, C. Hager-Braun, J. M. Binley, N. Schulke, H. Katinger, J. P. Moore, K. B. Tomer, *J. Virol.* **2001**, *75*, 10906.
[13] M. B. Zwick, R. Jensen, S. Church, M. Wang, G. Stiegler, R. Kunert, H. Katinger, D. R. Burton, *J. Virol.* **2005**, *79*, 1252.
[14] F. M. Brunel, M. B. Zwick, R. M. Cardoso, J. D. Nelson, I. A. Wilson, D. R. Burton, P. E. Dawson, *J. Virol.* **2006**, *80*, 1680.
[15] R. Bures, A. Gaitan, T. Zhu, C. Graziosi, K. M. McGrath, J. Tartaglia, P. Caudrelier, R. El Habib, M. Klein, A. Lazzarin, D. M. Stablein, M. Deers, L. Corey, M. L. Greenberg, D. H. Schwartz, D. C. Montefiori, *AIDS Res. Hum. Retroviruses* **2000**, *16*, 2019.
[16] F. Gao, E. A. Weaver, Z. Lu, Y. Li, H. X. Liao, B. Ma, S. M. Alam, R. M. Scearce, L. L. Sutherland, J. S. Yu, J. M. Decker, G. M. Shaw, D. C. Montefiori, B. T. Korber, B. H. Hahn, B. F. Haynes, *J. Virol.* **2005**, *79*, 1154.
[17] C. Grundner, T. Mirzabekov, J. Sodroski, R. Wyatt, *J. Virol.* **2002**, *76*, 3511.
[18] G. Ofek, M. Tang, A. Sambor, H. Katinger, J. R. Mascola, R. Wyatt, P. D. Kwong, *J. Virol.* **2004**, *78*, 10724.
[19] O. Lenz, M. T. Dittmar, A. Wagner, B. Ferko, K. Vorauer-Uhl, G. Stiegler, W. Weissenhorn, *J. Biol. Chem.* **2005**, *280*, 4095.
[20] R. M. Cardoso, M. B. Zwick, R. L. Stanfield, R. Kunert, J. M. Binley, H. Katinger, D. R. Burton, I. A. Wilson, *Immunity* **2005**, *22*, 163.
[21] S. Sanchez-Martinez, M. Lorizate, K. Hermann, R. Kunert, G. Basanez, J. L. Nieva, *FEBS Lett.* **2006**, *580*, 2395.
[22] S. Sanchez-Martinez, M. Lorizate, H. Katinger, R. Kunert, J. L. Nieva, *AIDS Res. Hum. Retroviruses* **2006**, *22*, 998.
[23] B. K. Brown, N. Karasavvas, Z. Beck, G. R. Matyas, D. L. Birx, V. R. Polonis, C. R. Alving, *J. Virol.* **2007**, *81*, 2087.
[24] Z. Beck, N. Karasavvas, J. Tong, G. R. Matyas, M. Rao, C. R. Alving, *Biochem. Biophys. Res. Commun.* **2007**, *354*, 747.
[25] C. R. Alving, Z. Beck, N. Karasavva, G. R. Matyas, M. Rao, *Mol. Membr. Biol.* **2006**, *23*, 453.
[26] B. F. Haynes, J. Fleming, E. W. St Clair, H. Katinger, G. Stiegler, R. Kunert, J. Robinson, R. M. Scearce, K. Plonk, H. F. Staats, T. L. Ortel, H. X. Liao, S. M. Alam, *Science* **2005**, *308*, 1906.

[27] S. M. Alam, M. McAdams, D. Boren, M. Rak, R. M. Scearce, F. Gao, Z. T. Camacho, D. Gewirth, G. Kelsoe, P. Chen, B. F. Haynes, *J. Immunol.* **2007**, *178*, 4424.
[28] G. Zeder-Lutz, J. Hoebeke, M. H. Van Regenmortel, *Eur. J. Biochem.* **2001**, *268*, 2856.
[29] N. Schulke, M. S. Vesanen, R. W. Sanders, P. Zhu, M. Lu, D. J. Anselma, A. R. Villa, P. W. Parren, J. M. Binley, K. H. Roux, P. J. Maddon, J. P. Moore, W. C. Olson, *J. Virol.* **2002**, *76*, 7760.
[30] Z. S. Qiao, M. Kim, B. Reinhold, D. Montefiori, J. H. Wang, E. L. Reinherz, *J. Biol. Chem.* **2005**, *280*, 23138.
[31] M. Kim, Z. Qiao, J. Yu, D. Montefiori, E. L. Reinherz, *Vaccine* **2007**, *25*, 5102.
[32] E. M. Scherer, M. B. Zwick, L. Teyton, D. R. Burton, *AIDS* **2007**, *21*, 2131.
[33] S. M. Alam, R. M. Scearce, R. J. Parks, K. Plonk, S. G. Plonk, L. L. Sutherland, M. K. Gorny, S. Zolla-Pazner, S. Vanleeuwen, M. A. Moody, S.-M. Xia, D. C. Montefiori, G. D. Tomaras, K. J. Weinhold, S. A. Karim, C. B. Hicks, H. X. Liao, J. Robinson, G. M. Shaw, B. F. Haynes, *J. Virol.* **2008**, *82*, 115.
[34] Z. Y. Sun, K. J. Oh, M. Kim, J. Yu, V. Brusic, L. Song, Z. Qiao, J. H. Wang, G. Wagner, E. L. Reinherz, *Immunity* **2008**, *28*, 52.
[35] C. R. Alving, *AIDS* **2008**, *22*, 649.
[36] H. Mozsolits, M.-I. Aguilar, *Biopolymers* **2002**, *66*, 3.
[37] R. B. Gennis, *Biomembranes: Molecular Structure and Function*, Springer, New York, **1989**.
[38] R. C. Aloia, H. Tian, F. C. Jensen, *Proc. Natl. Acad. Sci. USA* **1993**, *90*, 5181.
[39] B. Brügger, B. Glass, P. Haberkant, I. Leibrecht, F. T. Wieland, H.-G. Kräusslich, *Proc. Natl. Acad. Sci. USA* **2006**, *103*, 2641.
[40] *Biacore T100 Software Handbook*, Version AB, Biacore AB, 75450 Uppsala Sweden, **2006**.
[41] H. Mozsolits, T. H. Lee, A. H. Clayton, W. H. Sawyer, M.-I. Aguilar, *Eur. Biophys. J.* **2004**, *33*, 98.
[42] H. Nakamura, *Q. Rev. Biophys.* **1996**, *29*, 1.
[43] P. Zhu, J. Liu, J. Bess, Jr., E. Chertova, J. D. Lifson, H. Grise, G. A. Ofek, K. A. Taylor, K. H. Roux, *Nature* **2006**, *441*, 847.
[44] J. Liu, A. Bartesaghi, M. J. Borgnia, G. Sapiro, S. Subramaniam, *Nature* **2008**, *455*, 109.
[45] G. Zanetti, J. A. Briggs, K. Grunewald, Q. J. Sattentau, S. D. Fuller, *PLoS Pathog.* **2006**, *2*, e83.
[46] T. Suarez, W. R. Gallaher, A. Agirre, F. M. Goni, J. L. Nieva, *J. Virol.* **2000**, *74*, 8038.
[47] S. Shnaper, K. Sackett, S. A. Gallo, R. Blumenthal, Y. Shai, *J. Biol. Chem.* **2004**, *279*, 18526.
[48] R. L. Rich, D. G. Myszka, *Trends Microbiol.* **2003**, *11*, 124.
[49] A. S. Veiga, M. A. Castanho, *Antiviral Res.* **2006**, *71*, 69.
[50] D. J. Schibli, R. C. Montelaro, H. J. Vogel, *Biochemistry* **2001**, *40*, 9570.
[51] M. Lorizate, A. Cruz, N. Huarte, R. Kunert, J. Perez-Gil, J. L. Nieva, *J. Biol. Chem.* **2006**, *281*, 39598.
[52] C. Luo, K. Wang, D. Q. Liu, Y. Li, Q. S. Zhao, *Cell. Mol. Immunol.* **2008**, *5*, 1.
[53] M. B. Zwick, *AIDS* **2005**, *19*, 1725.
[54] N. Huarte, M. Lorizate, R. Maeso, R. Kunert, R. Arranz, J. M. Valpuesta, J. L. Nieva, *J. Virol.* **2008**, *82*, 8986.
[55] G. Frey, H. Peng, S. Rits-Volloch, M. Morelli, Y. Cheng, B. Chen, *Proc. Natl. Acad. Sci. USA* **2008**, *105*, 3739.
[56] S. A. Vishwanathan, E. Hunter, *J. Virol.* **2008**, *82*, 5118.
[57] S. Phogat, K. Svehla, M. Tang, A. Spadaccini, J. Muller, J. Mascola, I. Berkower, R. Wyatt, *Virology* **2008**, *373*, 72.
[58] G. B. Fields, R. L. Noble, *Int. J. Pept. Protein Res.* **1990**, *35*, 161.
[59] H. Franzén, L. Grehn, U. Ragnarsson, *J. Chem. Soc. Chem. Commun.* **1984**, *24*, 1699.
[60] Y. N. Abdiche, D. G. Myszka, *Anal. Biochem.* **2004**, *328*, 233.

Received: September 9, 2008
Published online on March 12, 2009

